Dynamic Models for Plasma-Wall Interactions

A.Yu. Pigarov (UCSD)

P. Krstic (ORNL), S. Krasheninnikov (UCSD),

R. Doerner (UCSD),T. Rognlien (LLNL)

13th Plasma Edge Theory workshop

September 2011, Lake Tahoe, CA

Outline

Physics of plasma-wall interactions will be discussed as it enters our models and modeling results

-> Introduction

-> Hierarchy of models used in PMI

-> Macroscopic transport models

-> Modeling of deuterium recycling, retention, chemical erosion, RES

-> Classical MD modeling

-> Quantum TBDFT modeling

-> Dynamic plasma-wall coupling

-> Modeling of plasma-wall under intermittent non-diffusive plasma transport

Role of Plasma-Wall Interactions

Design:

Plasma power load handling
Erosion rates
PFS component s lifetime
Diagnostics lifetime
Material degradation

Plasma performance:

Core plasma contamination with impurities
Plasma performance degradation when wall switches to gas release
Thermal instabilities, MARFE formation, disruptions caused by PMI

Burn control:

Density and profile control
D/T isotope composition control
He ash removal

Safety:

Tritium retention and permeation
Dust production

PMI processes

Phenomena	Process
Recycling	Implantation Desorption Adsorption Emission Trapping/de-trapping Chemical reactions, molecular physics Back scattering
Erosion	Physical sputtering Chemical sputtering RES Thermal sublimation
Damage	Surface modification Creation of traps
Heating	Heat transfer Thermal radiation Melting Surface modification
Re-deposition	Soft carbon film Hard a-C:H films Mixed materials

Plasma-wall interaction conditions

-> Different materials Be, C, W, Li and species D/T, He, O, Ar
-> Plasma fluxes are strongly varying in time and along the surface
->Transitional events: plasma intermittency due to blobs, ELMs
-> Disruptions, L-H mode transitions
-> High erosion/deposition rates, phase transitions, chemistry, Co-deposition, film growth, fuzzy structure formation, dust

-> strong operational and safety limits in fusion devices

-> collision dominated implantation region
If $\Phi_{peak}=10^{21}/cm^2/s$ then each surface atom will be hit by plasma ion in a microsecond; very far from thermal equilibrium
-> slow evolution of bulk of material

All PMI areas are important and all are the dynamic processes at different time scales -> dynamic models are needed

Hierarchy of “wall” models

Quantum Chemistry & MD

->models based on DensityFunctionalTheory(DFT)
->Tight binding theory (TB)
->Classical Molecular Dynamics (MD)
->Embedded Atom Model (EAM)
->hybrid models:
Quantum(TBDFT)-classical MD (P. Krstic)
Car-Parrinello

Kinetic (MC) models

-> Hyper-dynamics (Voter)
-> Lattice defect formation (TRIM,MARLOW)
-> Surface modification under irradiation (TRYDIN, WBC,ERO)
-> Effects of 3D structure, anisotropic transport, material composition
->Porous media

Macroscopic transport

-> Transport of implanted particles
-> evolution of interstitial atoms, vacancies, dislocations, cracks, grain boundaries
-> chemistry
-> mixed materials
-> stress

Integration of models

A need in “fine-grained” models for proper modeling of PMI under fusion reactor conditions based on Quantum - Classical MD approach.

A need in Accelerated Dynamic model to extend Q-MD to microns and microsecond scales

A need in detailed macroscopic transport models bridging plasma and wall dynamics

General methods of integration:
-> Hybrid models
-> Adaptive domain decomposition
-> Framework for code integration
->Uncertainty analysis
->Validation&Verfication

Macroscopic transport models

-> First models for fusion were developed in ~1970 (Baskes)

->Models are based on consideration of species implanted into solids as solute interstitial gas

-> Solve a system of coupled equations for solute species transport and chemical reactions

$$\partial c_i/\partial t + \partial J_i/\partial x = c_j \nu_{j->i} - c_i \nu_l - c_i \nu_{i->j} + \alpha_{i->j} c_i c_j - \alpha_{j->i} c_i c_j + S_i$$

-> Two approaches to J:
Tracer (First Fick law)
Chemical (Second Fick Law)

-> need data on activation energies, rate coefficients etc. Those usually come from DFT-based modeling and experiment. However structure of implantation region is strongly modified that brings uncertainty

-> Distinguish the collisional and thermal terms
$\nu_{col}=\Sigma_i \sigma_{ij}(E(x),w)\Phi(x)$ $\nu_{th}=\nu_{base}$ exp(-E/kT) (Arhenius)

Stress field models

At high irradiation doses, implanted particles can propagate deep into material due to stress field.

Consider ideal isotropic elastic metallic matrix, the displacement vector only due to hydrogen concentration gradient is

$$\rho\partial^2\mathbf{x}\partial t^2 - Y/2(1-\nu)*\nabla^2\mathbf{x} - Y/2(1-\nu)(1-2\nu)*\nabla(\nabla\mathbf{x}) = -Y\beta/3(1-2\nu)*\nabla c$$

Inclusion stress field for alloy results in:

$$\rho\partial c\partial t+\partial J_i/\partial x_i=0$$

$$J_i=-\rho\partial M_{ij}\partial/\partial x_j \{\partial G/\partial c - a_{ij}\partial^2 c/\partial x_k\partial x_l + \partial/c[(\varepsilon_{kl}-\omega_{kl})C_{klrs}(\varepsilon_{rs}-\omega_{rs}]\}$$

increasing complexity and uncertainty
Wavy
Highly non-linear
Stochastic

However it is a way to go to describe long time scale consequences of plasma-wall interaction

Binodal/Spinodal decomposition

At large hydrogen concentrations the H-H interaction cannot be neglected.

Hydrogen transport in solution is due to gradient of chemical potential μ:
$j = -L\nabla\mu = -D(C)\nabla C, \quad D = L\partial\mu/\partial C$
Diffusion coefficient is function of hydrogen concentration as
$D(C) = D_o\{1 + [U/kT]\, C\, [1 - C/C_{max}]\}$
If U<0, then there is T at which D=0.

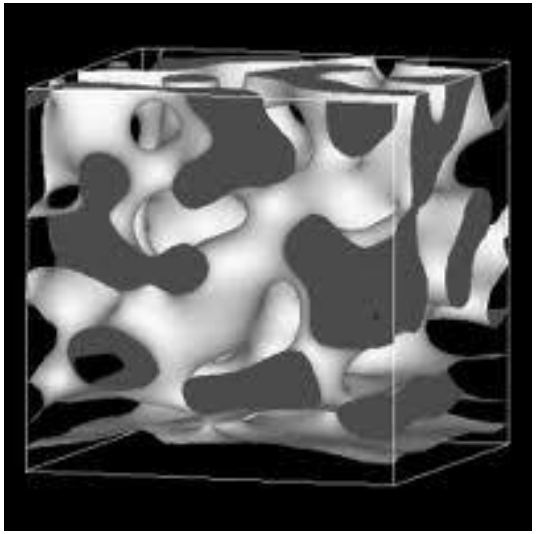

Has been studied for Pd-H system by L. Smirnov [Int. J. Hydrogen energy 1997]
$kT_s = -(U + A + 4B\, C^3)\, C\, (1 - C)$, A=0.05 ,B=0.5 eV

Stochastic effects are described by Cahn-Hillard theory. The chemical spinodal occurs when $\partial^2\mu/\partial x^2 < 0$. The state is unstable against small hydrogen density perturbations, the resulting solution is oscillatory and represents irregularities. Segregated domains grow in time as $t^{1/3}$.

WALLPSI model

->One-dimensional transport code for plasma particles and heat inside the wall

-> Provides dynamic calculations of featured defects, erosion rates and D retention and permeation

-> Designed to be a component in self-consistent core-edge-wall modeling

-> follows tracer approach for solute gas but includes collision terms, non-diffusive transport and moving plasma-facing interface

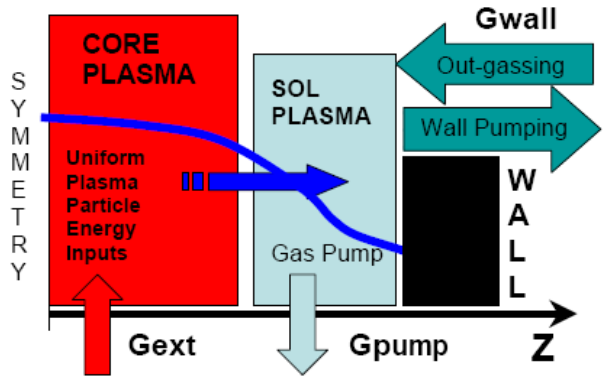

	D recycling	D retention	erosion	CHS	RES
Mobile D	+	+	+	+	
Ion-induced defects	+	+	+	+	+
Vacancies		+			+
Interstitial atoms		+	+		+
Lattice atoms			+	+	

Mobile deuterium under surface recombination limited conditions

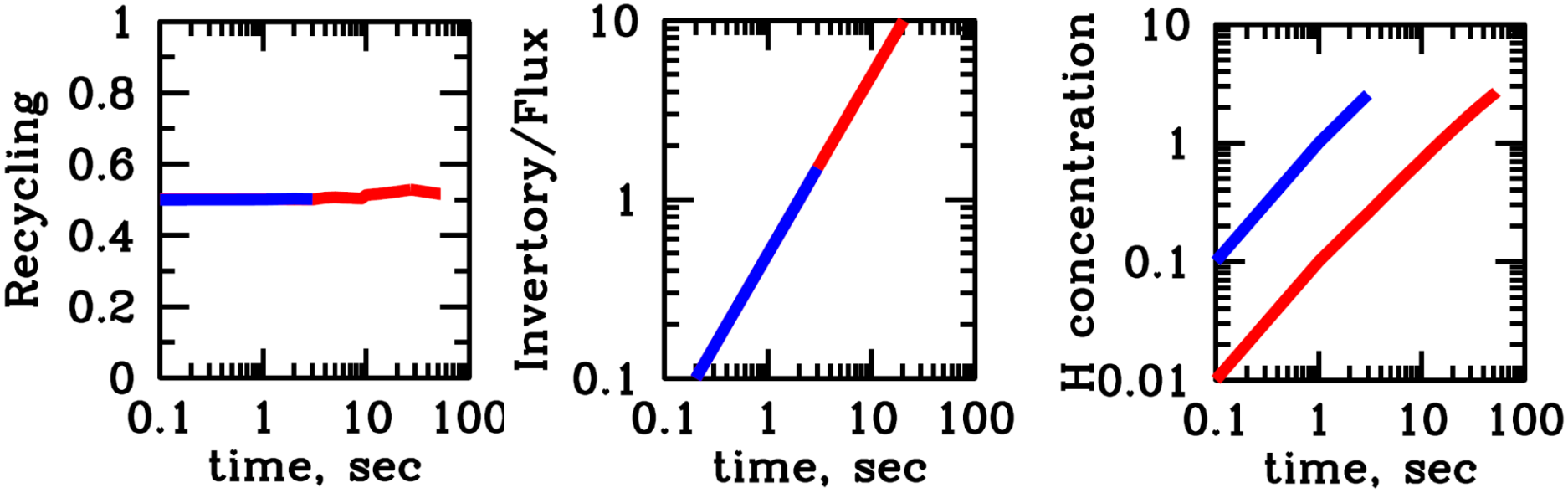

WallPSI calculations for D->Be, room temperature, Edes=0.8eV, Edif=0.5eV, $\Phi=10^{17}$/cm2 (**blue)** and10^{18}/cm2(**red**); Implantation energy is 75 eV.

->Recycling coefficient is close to backscattering coefficient

->Wall is continuously pumping, inventory increases linearly

->Concentration of mobile hydrogen attains its limit 4 cites per lattice atom within implantation region

Super-saturated layer formation

Creation of supersaturated layer can explain many experimental features

->Saturation of retained deuterium with increasing irradiation dose
->Unity recycling in divertors, reduced wall pumping in tokamaks
->High irradiation dose experiments on PISCES + formation of BeD2 phase

-> SSL may be unstable akin to Cahn-Hillard

Non-diffusive models for super –saturated layers:
->Local Mixing Model (Brice 1987)

->Convective transport

Convective transport model for SSL

Interpretation for irradiation induced convection:

->Incident particles produce wakes in matter through which mobile deuterium or volatile species can be advected or released.

->Mean free path of recoil particles is usually larger than cell size

->particles moving in wakes were observed in MD modeling of hydrogenated carbon bombardment (Krstic, priv.com)

->Lifetime of wakes is not investigated yet and may be from ps (sputtering) to ms (i.e. relaxation due to stress)

Model:

->The integral collisional term $K(x)=\sum_i \int f_i(x') T(x,x') dx'$
is replaced by approximate convective term $K(x)=d/dx\ N_m\ V_{conv}(x)$

->Introduce critical incident flux Φ_* at which $N_{max}V_*= \Phi_*$, where N_{max} is maximal concentration of mobile hydrogen.

->For $\Phi_*=10^{19}/cm^2/s$, $N_{max}=10^{23}/cm^3$, $V_* =10^{-4}cm/s$.

->$V_{conv}(x,t)=V_*\ \Phi(x,t)/\Phi_*= \Phi/N_{max}$, where $\Phi(x,t)$ is the depth "profile" of incident flux.

-> transport is non-local, depend on incident particle, energy and angle.

Continuity equation for SS layer:

$dN/dt= \Phi(1-R_n)/L_d - \Phi N/N_{max}/L_d$,

$N(t)/N_{max}= (1-R_n) - [1-R_n-N(t=0)/N_{max}] \exp(- \Phi N_{max}/L_d\, t)$

Equilibrium concentration is independent on flux.

Characteristic time to attain "collisional" equilibrium concentration is $\Phi N_{max}/L_d$

Mobile D in supersaturated layer

WALLPSI calculations for typical PISCES conditions:75eV D->Be, room temperature, incident flux $2x10^{18}/cm^2/s$.

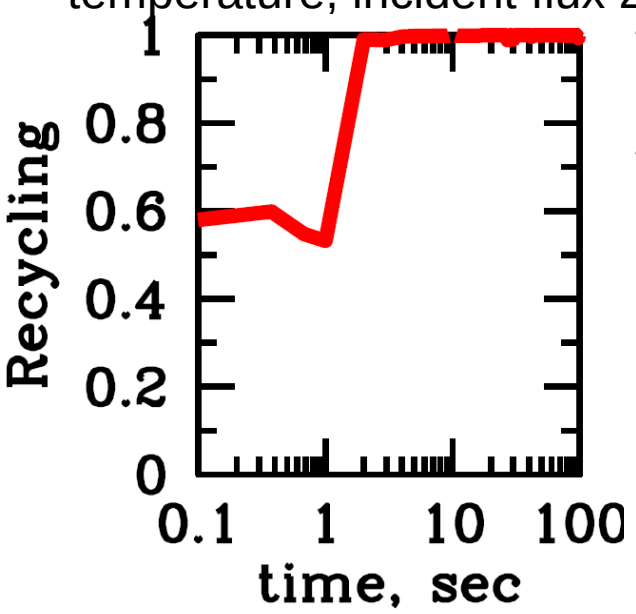

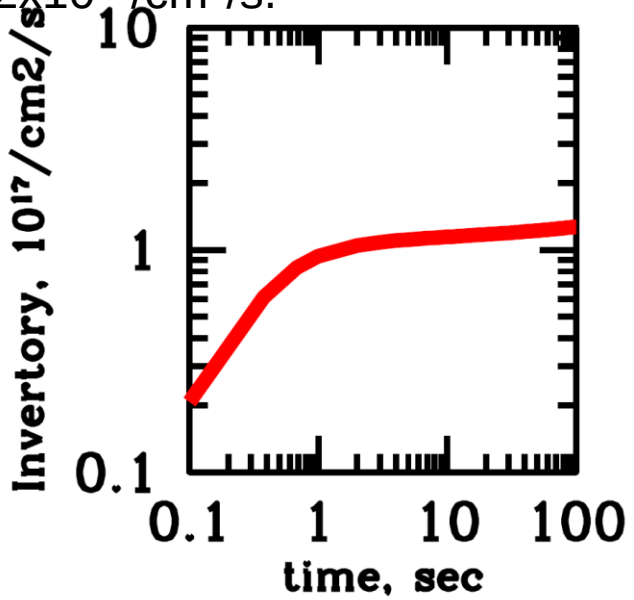

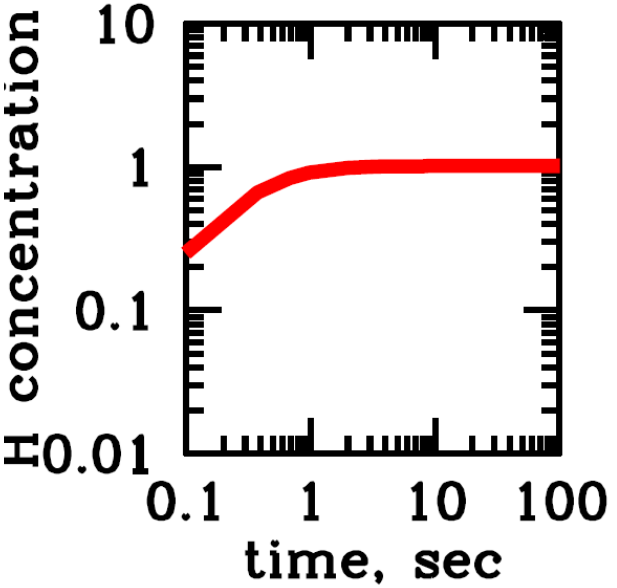

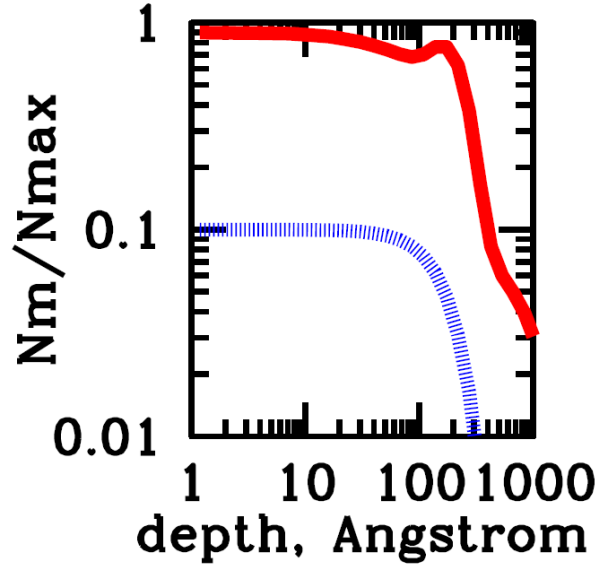

->Characteristic time for SSL is 1sec as expected
->D is well “confined” within SSL layer
->Unity recycling
->Slow diffusion into the bulk
->D is at measured retained level
-> Suggests strong dependence on incident energy via implantation range

Mobile D release from SSL

WALLPSI calculations for PISCES :75eV D->Be exposure at room temperature; flux 10^{19}/cm^2/s is turned off at 10sec. Edes=0.8eV, Edif=0.5eV

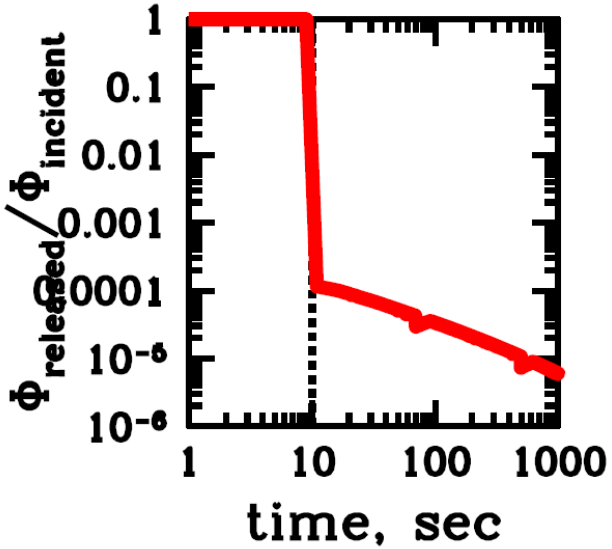

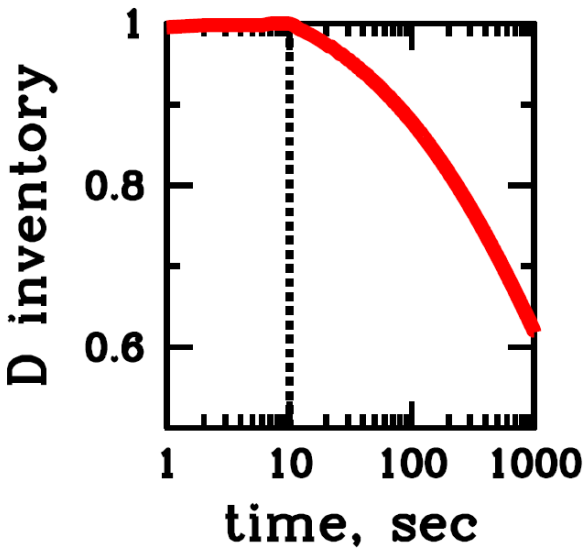

-> Releasing flux is at low level10^{14}-10^{15}/cm2/s for room temperature and recombinative desorbtion activation energy Edes=0.8eV

-> D inventory decreases 2x at 20 min timescale.

-> However it is hard to diagnose since after 2days when sample gets to TDS most of inventory is lost

->At room temperatures wall is capable of retaining significant amount of mobile D

->At higher temperatures initial D inventory is smaller as well as D release is much faster.

-> Cleaning discharges in tokamaks can be effective if low energy incident particles can release more D than deposit.

D permeation

In the current tokamaks deuterium permeation through tiles is small, no problems.

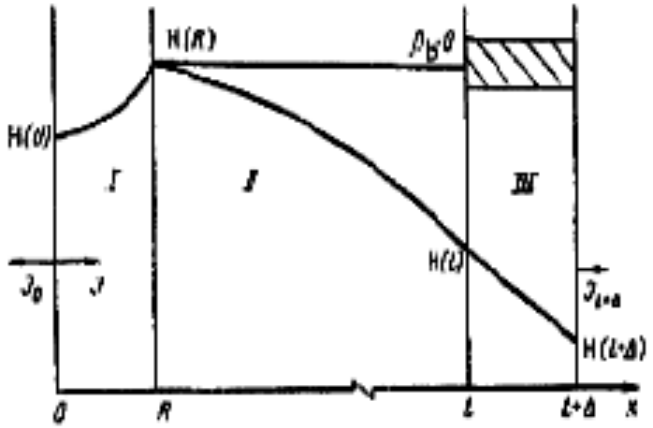

In the next-step devices, public safety sets limit on tritium leakage:
~1g/year
Usage of Be and high operational temperatures as well as transits promote permeation
Coolant faced surface may include Permeation Barriers

D traps

Intrinsic traps:

Vacancies and their clusters
Interstitial atoms and their clusters
Bubbles
Grain Boundaries
Pores

Ion-induced traps:

Voids
Add-atoms
Vacancies & interstitial atoms
via Bond breaking

Stress field induced traps

Fuzz (theory was recently developed by Krasheninnikov)
Dislocations and loops

Various models for these traps has been developed.

D traps in Be

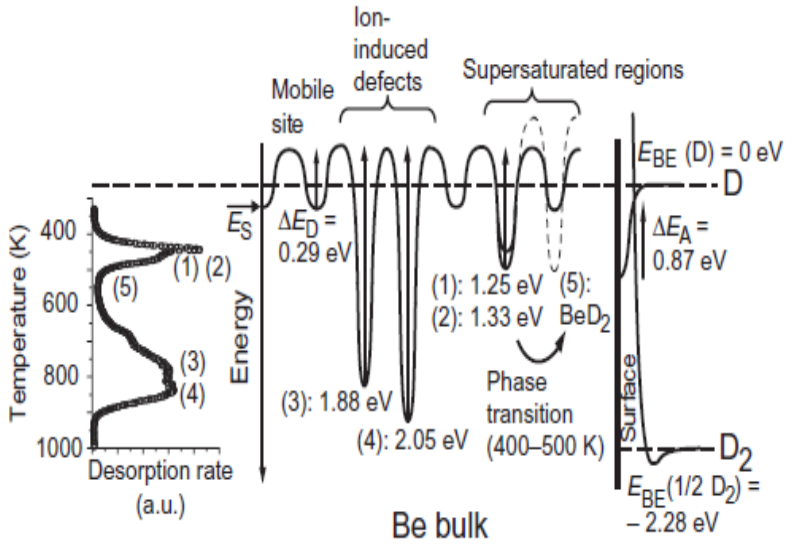

M Reinelt[1], A Allouche[2], M Oberkofler[1] and Ch Linsmeier[1,3]
New Journal of Physics **11** (2009) 043023

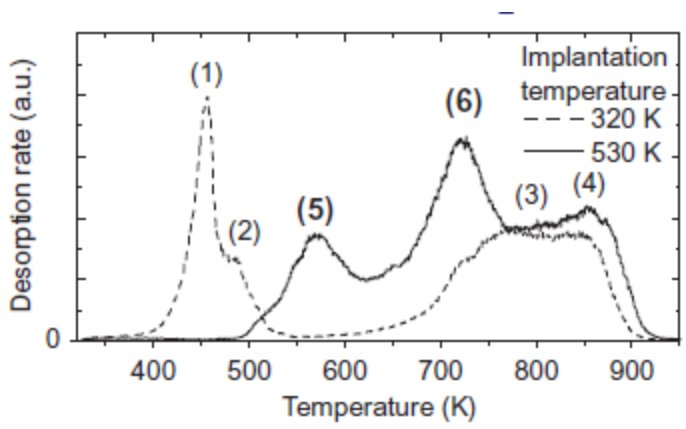

-> Thermal Desorption Spectroscopy (TDS) or Temperature Programmed Desorption (TPD) is the most informative diagnostic

->Data analysis by Reinhelt et.al with TMAP7 code has indentified the following D traps:

Ion-induced traps:1.88 and 2.05eV, (3)&(4)

Hydride traps 1.25 and 1.33eV, (1) &(2)

Impurities (Oxigen) (5)&(6)

->BeD2 decomposes with increasing temperature at 400-500K

-> Vacancies and interstitial atoms are also traps for D with binding energies ~1.2-1.5eV (Allouche et.al, JPC 2010)

Existing models suggest that concentration of traps is fixed, however dynamic model is needed

Chemistry in SSL for Be

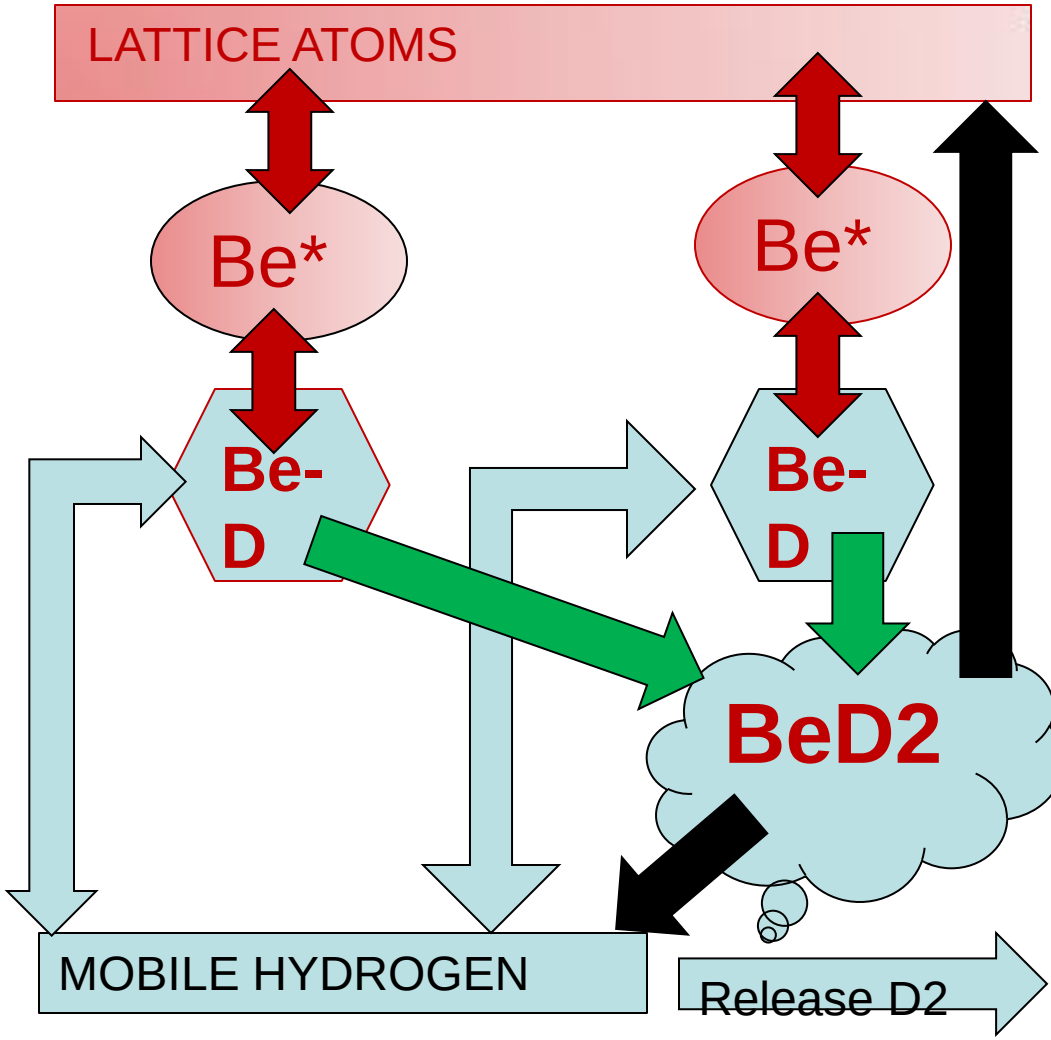

Creation chemically active atom by breaking bonds

Hydrogenation
Be*+D->Be-D

Agglomeration to BeD2
“Phase transition”

BeD2 decomposition
D2 release

Chemical kinetics model

$$dN_w/dt = (N_a-N_w)\nu_{a->w} - N_w\nu_{w->a} - (N_w-N_{hw}-N_{hy})\,(\nu_{spt,w}+\nu_{des,w}) - N_{hw}(\nu_{spt,hw}+\nu_{des,hw}) - N_{hw}(\nu_{spt,hy}+\nu_{des,hy})$$

$$dN_{hw}/dt = \alpha_{h,w}(N_w-N_{hw}-N_{hy})N_m - N_{hw}\nu_{hw->w} - \alpha_{hy}N_{hw}N_{hw} - N_{hw}\,(\nu_{spt,hw}+\nu_{des,hw}) + N_{hy}\nu_{hy->hw}$$

$$dN_{hy}/dt = \alpha_{hy}N_{hw}N_{hw} - N_{hy}\nu_{hy->hw} - N_{hy}(\nu_{spt,hy}+\nu_{des,hy}) - N_{hy}\nu_{hy->m}$$

$$dN_{m}/dt = -\alpha_{h,w}(N_w-N_{hw}-N_{hy})N_m + N_{hw}\nu_{hw->w} + N_{hy}(\nu_{spt,m}+\nu_{des,m}) + N_{hy}\nu_{hy->m} + \mathbf{S_m}$$

N_w -> **Be*** N_{hw}->**Be-D** N_{hy}->**BeD2** N_m-> **mobile D**

All species are dynamically coupled.
Collisional and thermal processes are equally important.
In equilibrium, D recycling between species is close to 1.

Generation of traps for D

WALLPSI calculations for 75eV D->Be at room temperature

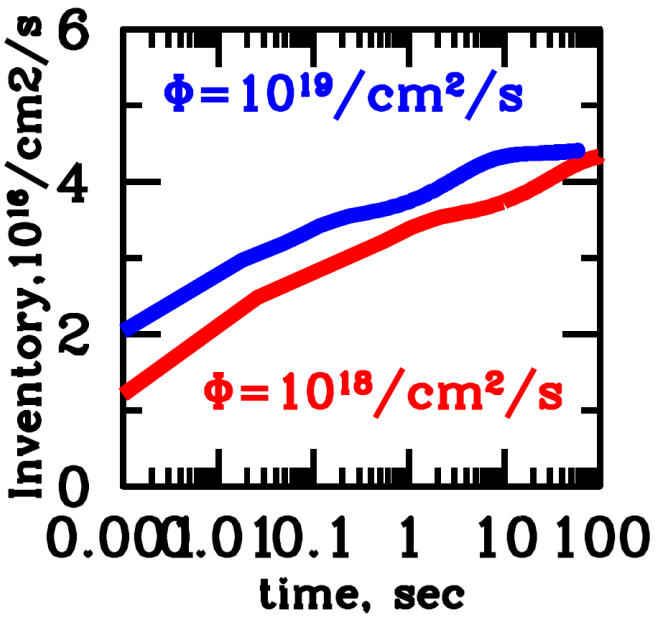

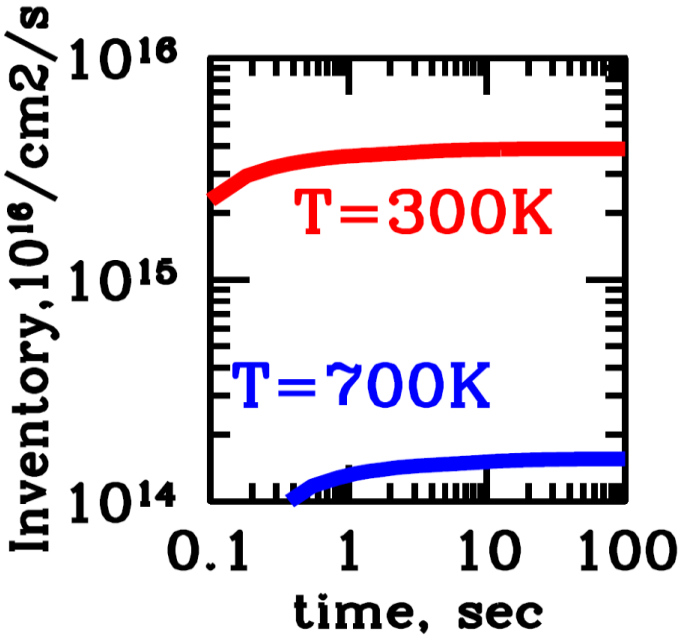

Broken Bond traps and Hydrates

Vacancies and recoil atoms

->Characteristic time for trap generation is determined by cross-section and flux
->Concentration of BB traps saturates at a minute timescale corresponding to D capacity2x4.5 10^{16}/cm2/s and weakly depending on wall temperature.
->Inventories of vacancies and recoils are equal and are small due to mutual annihilation. However, they contribute to D inventory at room temperatures because of 6-D-capacity.

Deuterium retention

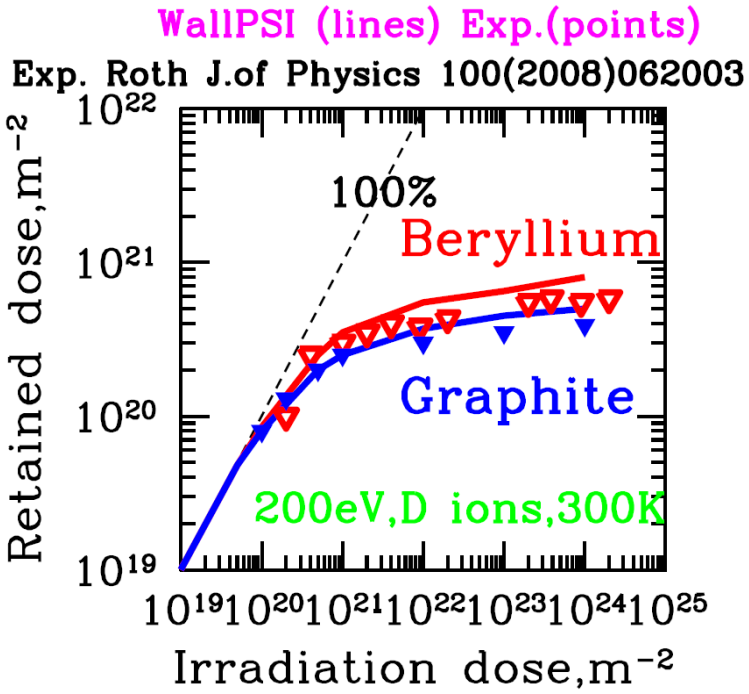

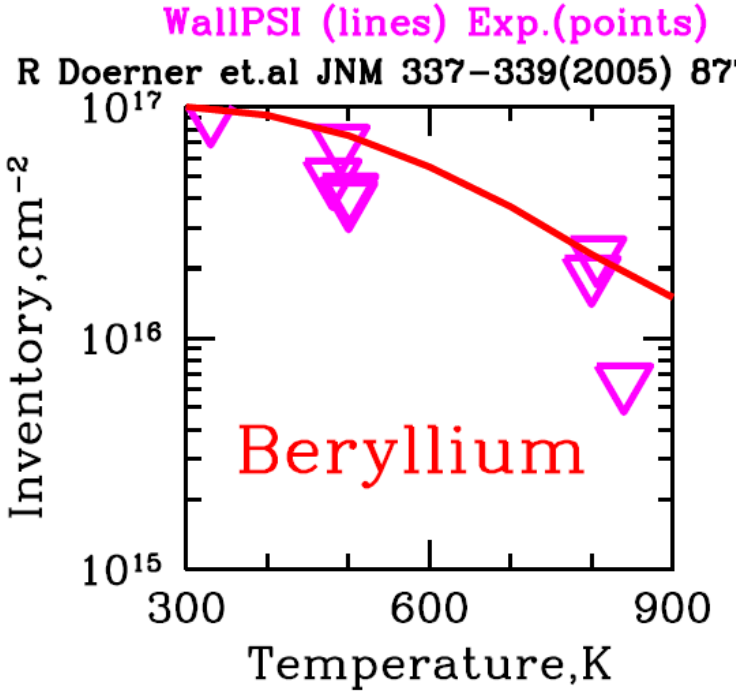

->Saturation is attained at lowdoses10^{17}/cm^2
->retained level is at 0.4 D per lattice atom
->most of D inventory is within implantation region
->retained D can be available during disruptions and type-I elms in ITER
-> note: mobile D is not counted here!

-> retained dose changes little at low temperatures <500K
->gas is released consequently:
from vacancies at ~400K
from hydrates at 500-700K
from BB traps at >700K
->consistent with TDS analysis

Chemical sputtering of Be

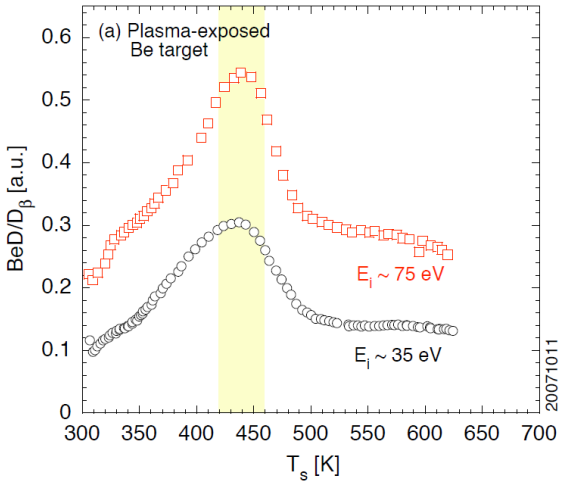

Courtesy of D. Nishijima

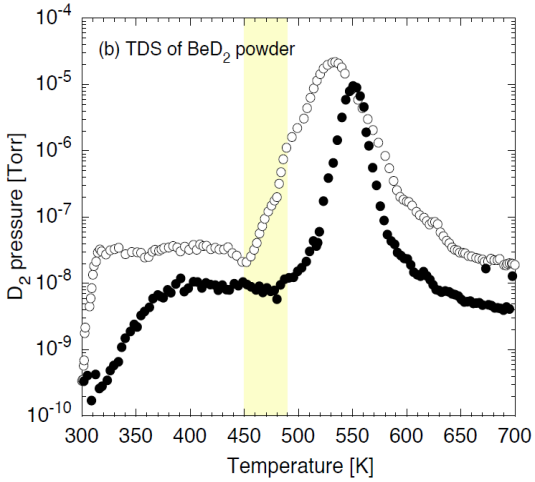

->Chemical sputtering of Be was studied on PISCES measuring BeD bands in plasma (Nishijima et al PPCF2008)

-> Y_{CHS} has featured peak in temperature dependence at 440K

-> Y_{CHS} decreases at T>450-500K where BeD2 decomposes

-> MD modeling (Bjorkas NJP2009) showed sputtering yields of few % with BeD2 fraction ~0.4 at E~75eV. Temperature dependence was not studied.

Chemical sputtering (cont.)

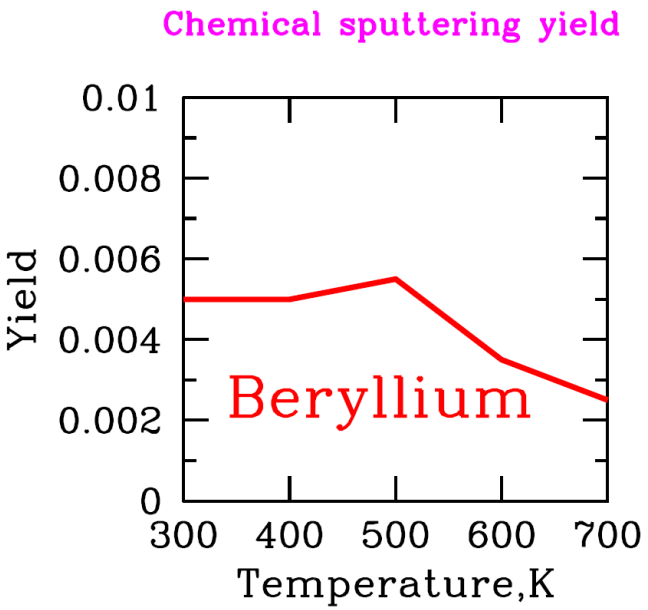

In proposed chain of chemical reactions, there are to two channels contributing to chemical sputtering:
-> physical sputtering of hydrogenated Be* (N_{hw}) and hydrides (N_{hy})
-> thermal desorption of these species

->At low T the main mechanism is direct sputtering
$Y_{CHS,collisional}=(N_{hy}+N_{hw})Y_{phys}/N_{as}$

-> There is small contribution from
$Y_{CHS,thermal}=N_{hy}\nu_{spt,hy}/\Phi$ (activation energy 0.9eV)

-> Decrease for T>500K is due to release of D. Consistent with retention modeling.

Radiation enhanced sublimation

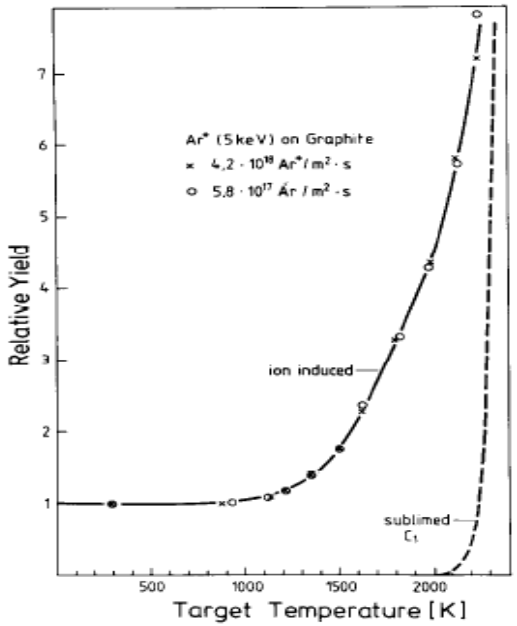

Journal of Nuclear Materials 155–157 (1988) 319–323

->RES was discovered in the ion beam experiments for carbon

-> Philipps (JNM 1995) proposed RES mechanism via release of mobile interstitial atoms of produced in the bulk due to bombardment

-> Modeled by many authors for carbon as transport of vacancies and interstitials

->this mechanism gives Y_{RES} be dependent on incident flux and species

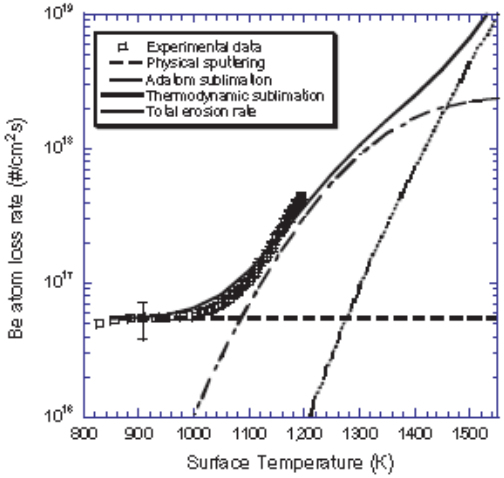

Journal of Nuclear Materials 337–339 (2005) 877–881

->High temperature release of Be atoms was also studied on PISCES (Doerner 2005)

->Experiment showed that no or small dependence Y_{RES} on flux and species

-> Add-atom mechanism for RES was proposed

RES modeling

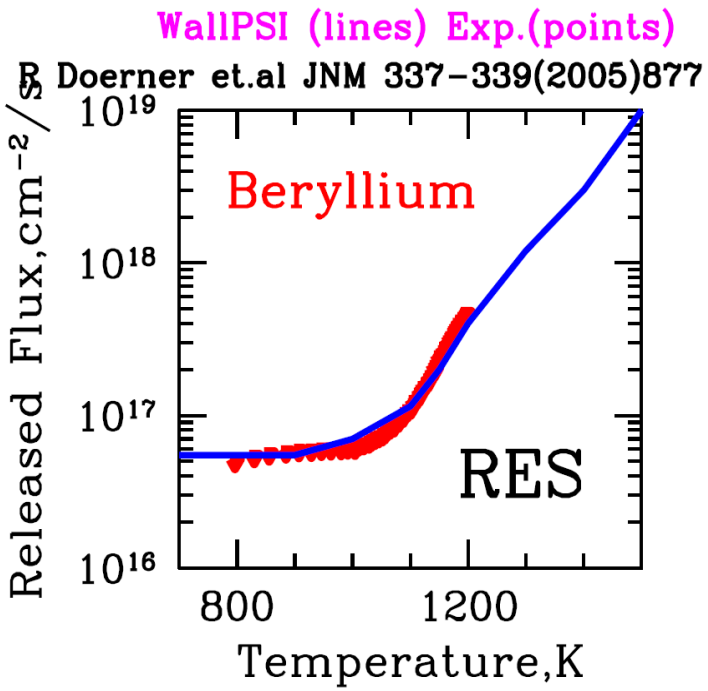

->Thermal desorption of “excited” atoms (or add-atoms) from surface is the main mechanism for RES in Be, whereas interstitial atoms produced in volume largely recombine with vacancies

$(N_{as}-N_w)\sigma_{a->w}\Phi=N_w(\sigma_{a->w}\Phi+\nu_{des}+\nu_{ds})$

$Y_{RES}=N_w\,\nu_{des}/\Phi$

$=N_{as}\,\sigma_{a->w}\,\nu_{des}/(\sigma_{a->w}\Phi+\nu_{des}+\nu_{ds})$

->At high temperatures, $Y_{RES}=N_{as}\sigma_{a->w}$ is independent on incident the flux Φ and species.

->At threshold T, $Y_{RES}\sim\exp(-E_{RES}/T)$

$E_{RES}=E_w=1.9$eV agrees with DFT calculations.

->Add-atom theory is in good agreement with PISCES experiments and with modeling by other authors.

->For carbon, experiments showed $E_{RES}=0.72$eV suggesting that interstitial/vacancy mechanism occurs

As in CHS, collisional and thermal processes are strongly coupled in dynamic RES loop

Synergistic effects in PMI

Reviewed in 1984 !!! by J. Roberto (ORNL) and R. Behrisch (IPPP), JNM

PMI processes are not a linear functional of plasma particles, power/particle fluxes, wall temperature, discharge history etc.

Adequate dynamic models are needed to include, at least, most important effects as well as to predict new ones.

Synergy #4.
Effect of multi-species particle fluxes

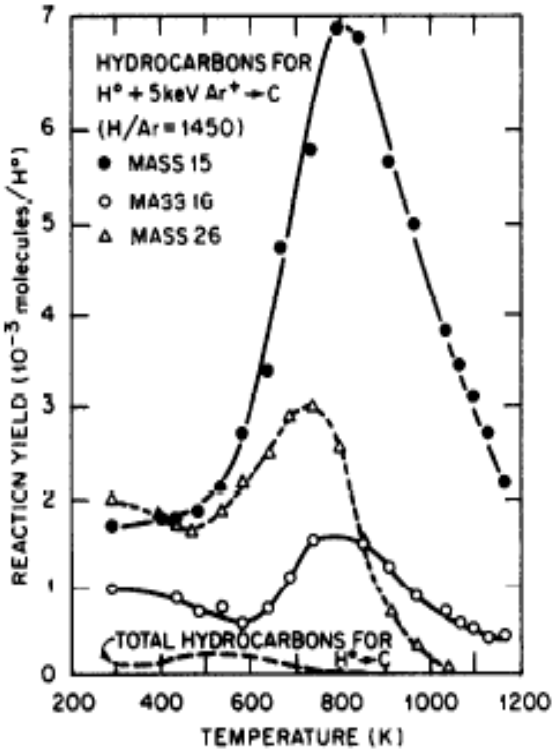

Fig. 3. Temperature dependence of the reaction probability (molecules/H-atom) for a graphite surface exposed to thermal atomic hydrogen with and without simultaneous bombardment by 5 keV Ar^+ ions. For the simultaneous bombardment measurements, the relative H to Ar flux was 1450. (after Vietzke et al. [56].)

Classical MD is based on inter-atomic potential model

Most advanced: hydro-carbon potential developed for chemistry

- Brenner, 1990 , 2002 : REBO, short range, 0.2nm
- more sophisticated AIREBO (Stuart, 2000, 2004, 1.1 nm)
- > 400 semi-empirical parameters, “bond order”, chemistry

$$\mathbf{F} = m\mathbf{a} \qquad \mathbf{F} = -\nabla U \qquad U = \sum_{i,j} V_{rep}(r_{ij}) - b_{ij}(r_{ij}) V_{attr}(r_{ij})$$

EXP!!

Adaptive Intermolecular Reactive Bond Order (AIREBO) potential : torsion, dispersion, Van der Waals,

EX: MD calc. of reflection coeff.

- Significant sensitivity to changes in potential model for some processes
- Experimental validation essential to establish credible MD simulation.
- Interatomic potentials for W and Be are less mature than for carbon and require more experimental validation.

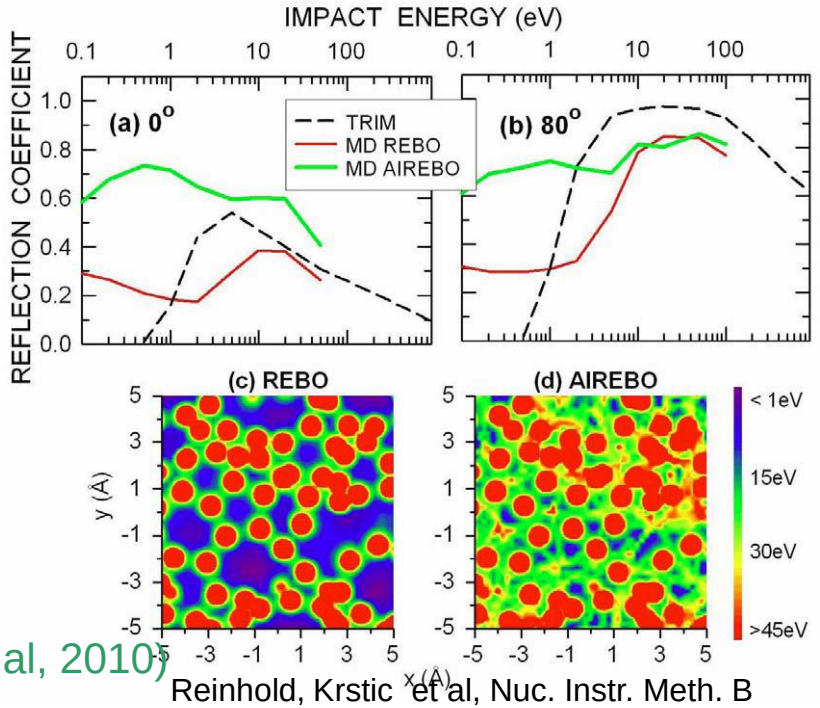

Reinhold, Krstic et al, Nuc. Instr. Meth. B 267, 691 (2009).

Improvements to CH potentials done (Kent Krstic et al, 2010)
New Li-C-H potentials being developed
(Dadras, Krstic et al, 2010)

MD modeling of evolution to D-supersaturated layer conditions

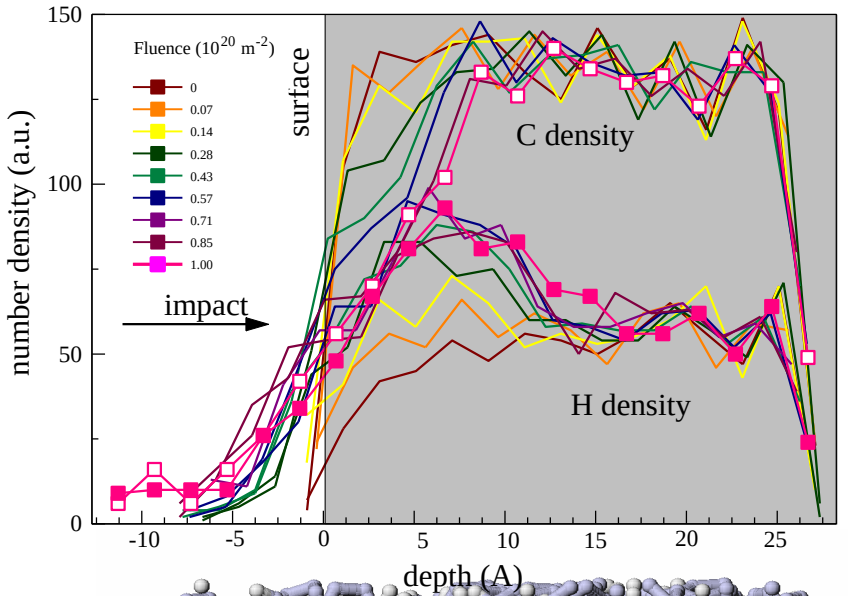

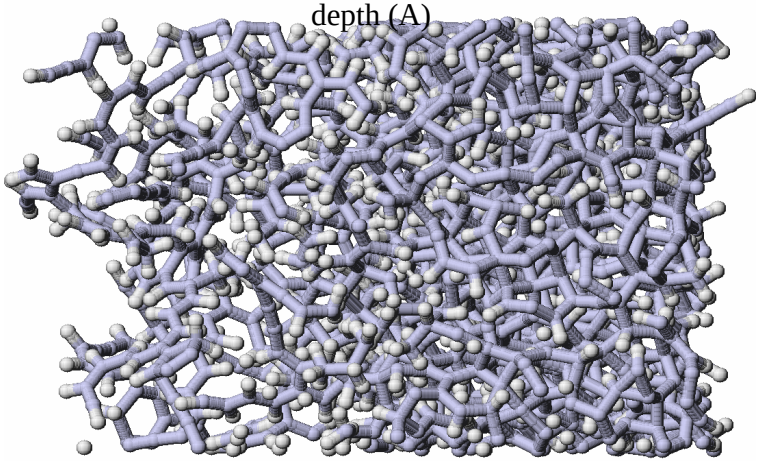

Stuart et al, J. Phys. Conf. Ser. 194, 012059 (2009)

- Surface supersaturated with D
- Lower C density at surface
- D/C ~1-1.5 at surface
- "Steady state" achieved by fluence of ~0.5 × 10^{20} m^{-2}
- Surface depth ~20 Å

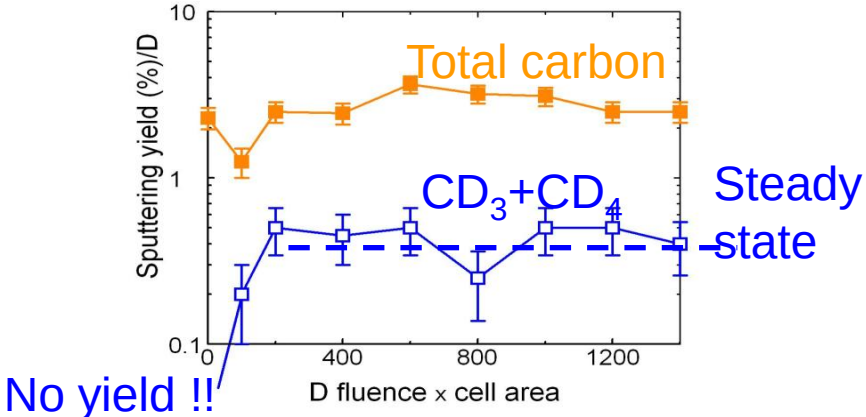

Dependence of Carbon erosion on the surface temperature

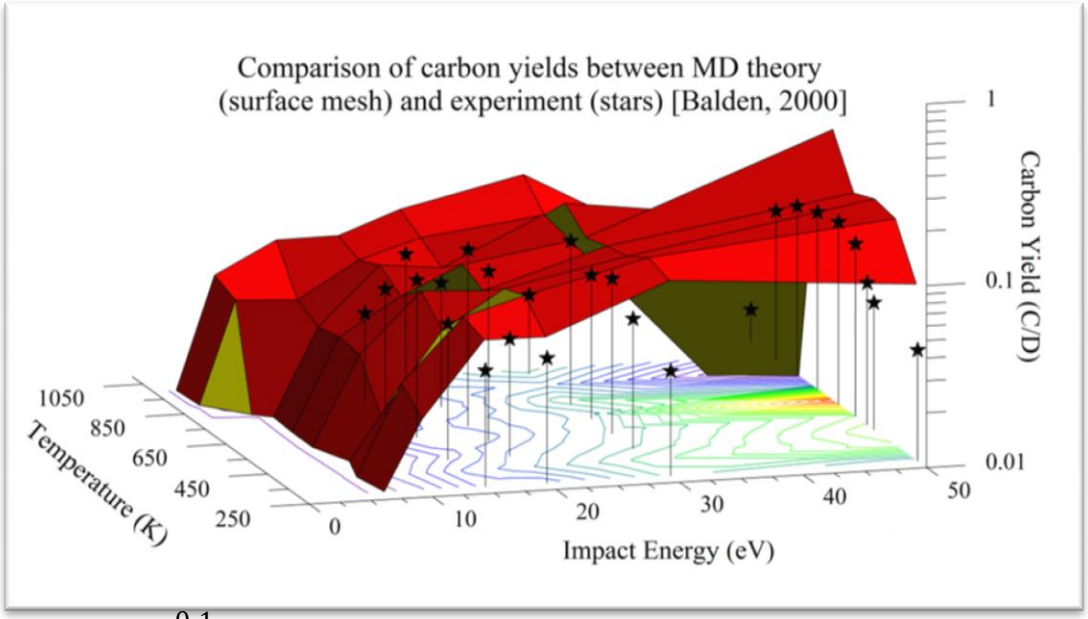

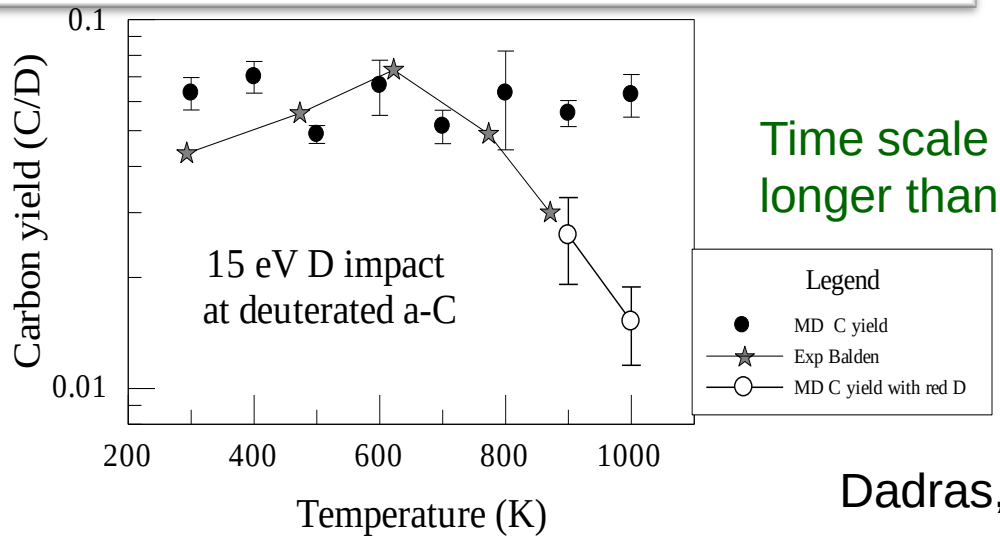

Time scale of thermal D-release longer than ps-ns scale

Dadras, Krstic et al, 2010

Rovibrational energy distributions: Ejected Hydrocarbons

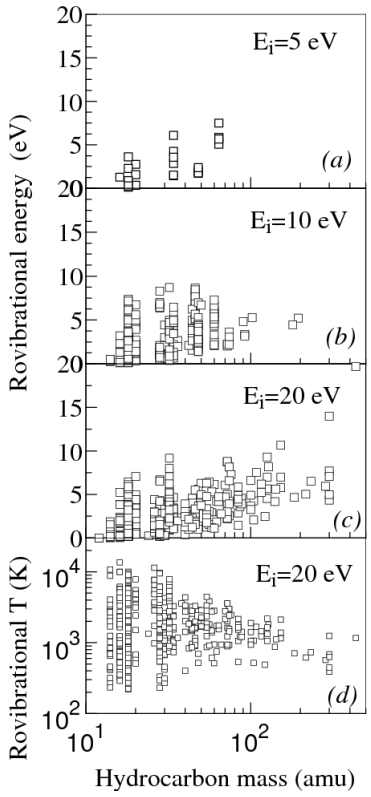

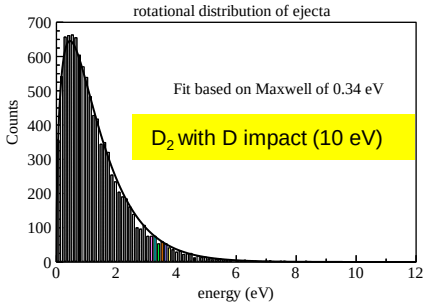

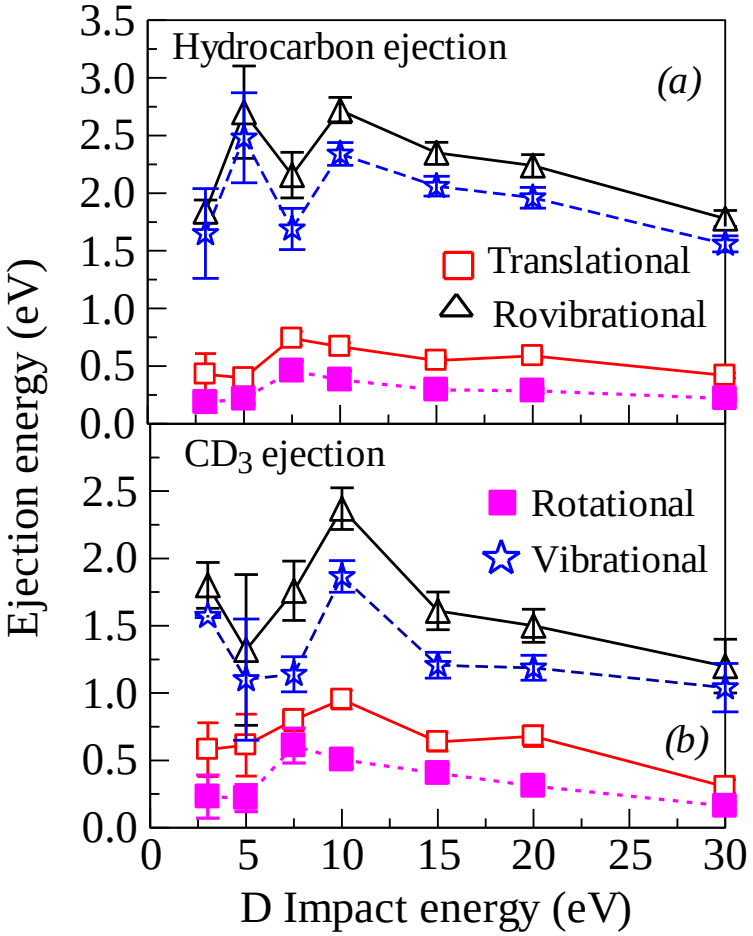

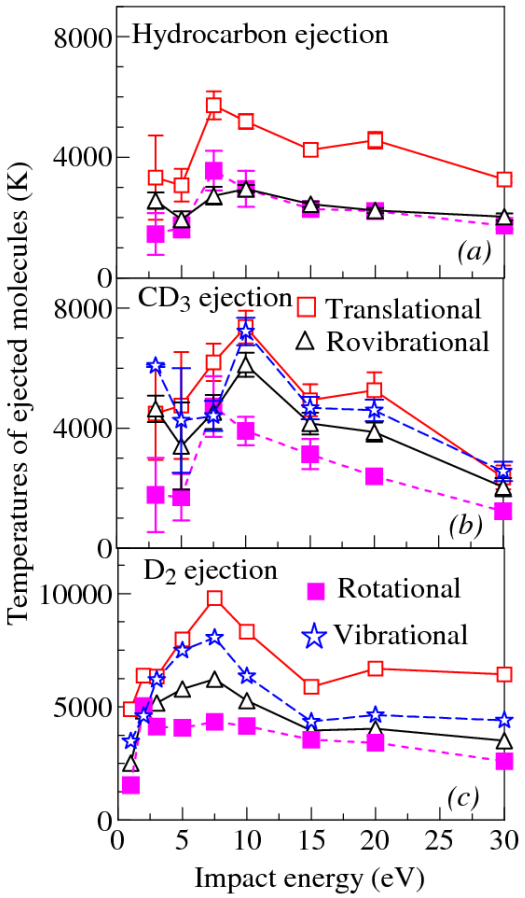

Ejection energy

Ejection temperature

Approximate thermalization indicated

Functions of hydrocarbon mass and impacting D energy

Krstic et al, J. Appl. Phys. 104, 103308 (2008).

Lithium dynamics: Problem to study theoretically because Li polarizing features when interacting with other elements

Electronegativity is chemical property of an element defining its tendency to attract electrons: Li has it exceptionally low in comparison to H , C, O, Mo, W.

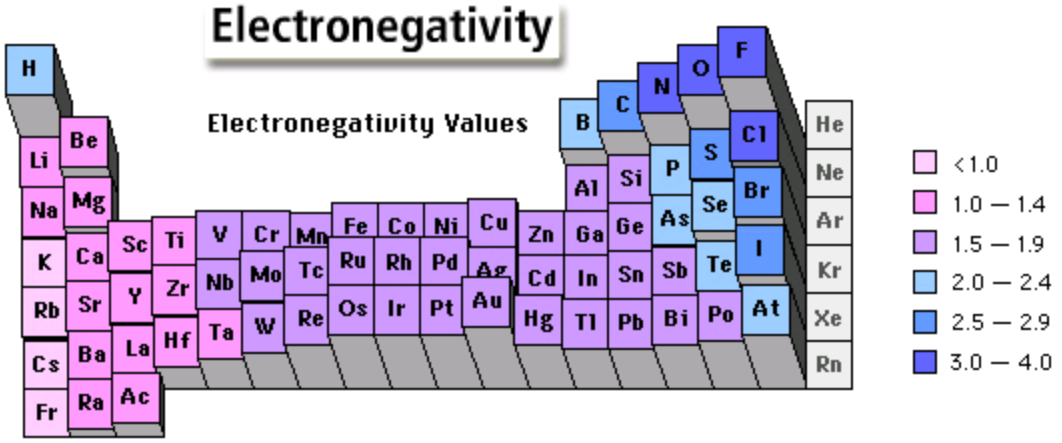

Consequence: Bonding between Li and other atoms covalent and polar;
Long-range nonbonding:
Coulomb :1/R
Lennard-Jones :$1/R^6$, $1/R^{12}$

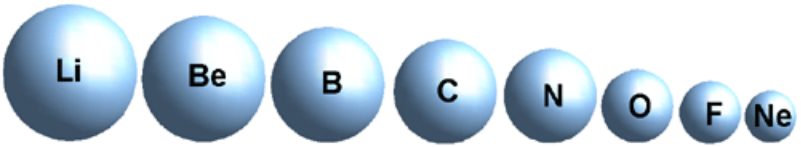

Electronegativity and size of atoms related!

Quantum-mechanical simulation of deuterium impact to lithiated and oxidated carbon surface

Employed the **Self-Consistent-Charge Density-Functional Tight-Binding (SCC-DFTB**) method (developed, by Bremen Center for Computational Materials Science, Germany) Parameterization due to K Morokuma. Kyoto-Emory

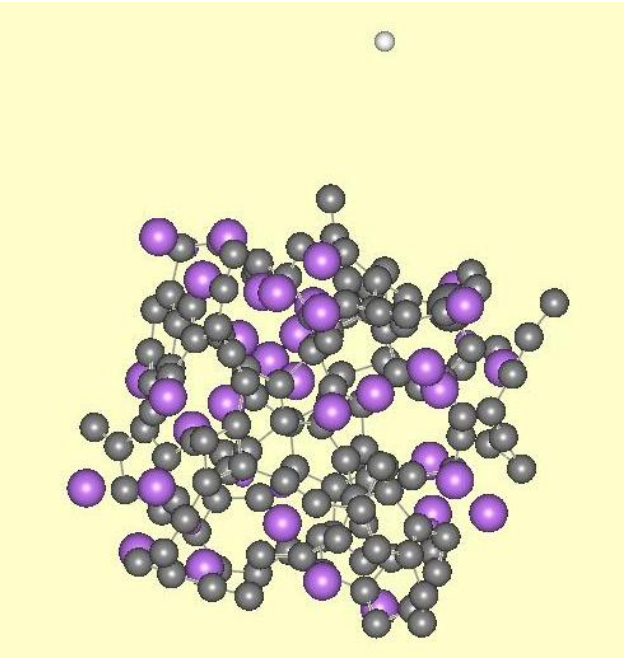

- Cell of **a few hunreds of atoms** of lithiated and oxidated amorphous carbon (~30% of Li, < 10% of O), at **300K**
- By random seed of Li and O in **amorphous carbon** and **energy minimization**, followed by thermalization
- bombarded by **5 eV D** atoms and **2.5 eV H**,
- **Perpendicularly** to the shell interface
- 5004 **random trajectories**

The cell swelled during the structure optimization

5004 processors of Cray XT5 (Jaguar, Kraken),
Time step 0.2-1fs, 24 hours: 200-400 fs.
One run over 120,000 CPU hours (TeraGrid project)

Final distribution of charges for retained D (H) atoms reveals the dominant chemistry

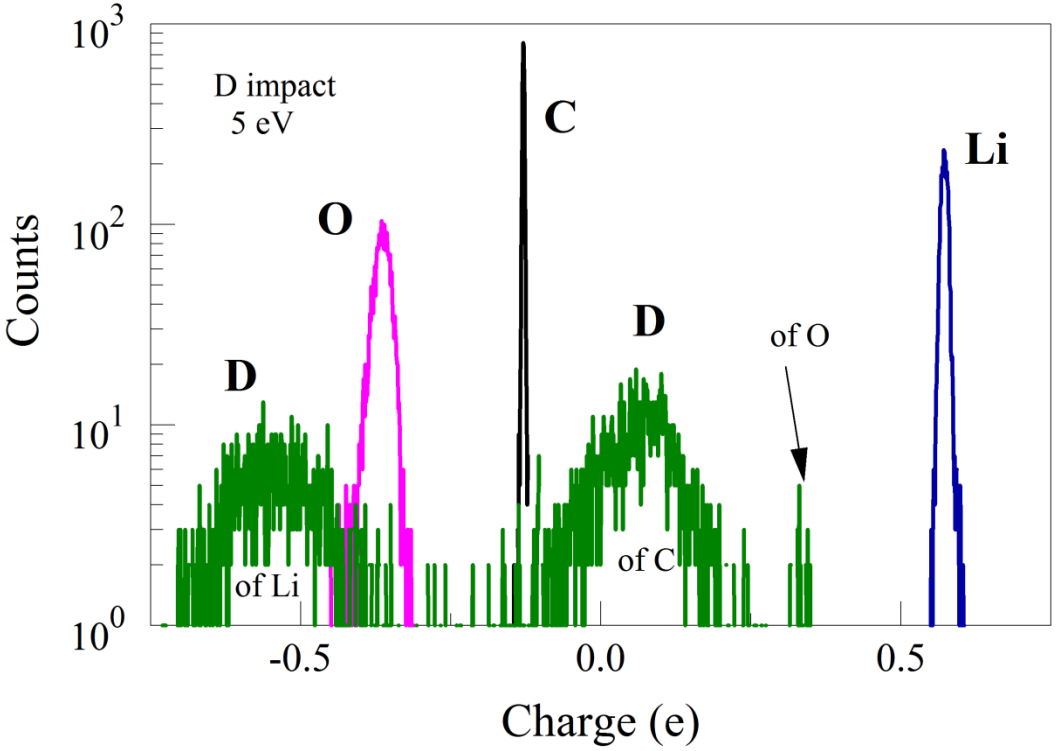

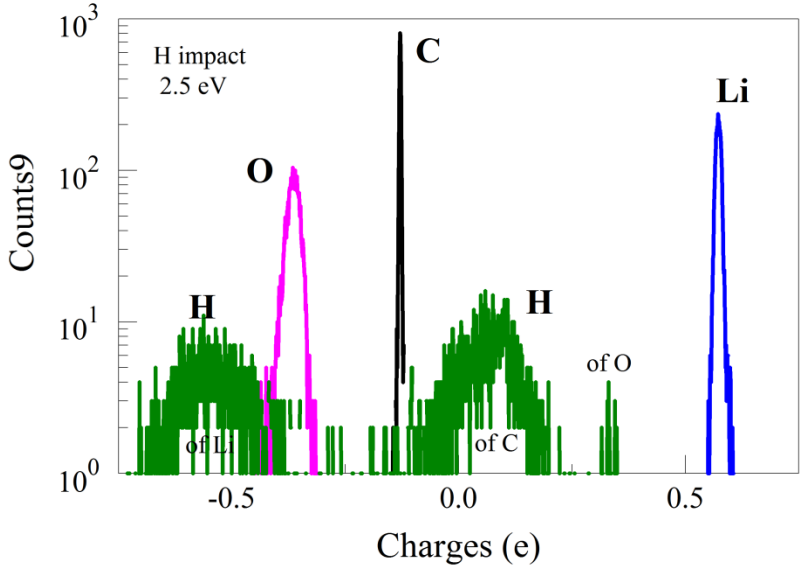

No isotope effect for chemistry (also found in D on C-H)

Large percentage of impact D (40%) prefer closeness of Li to settle down Not much attention to O (already bonded to Li)

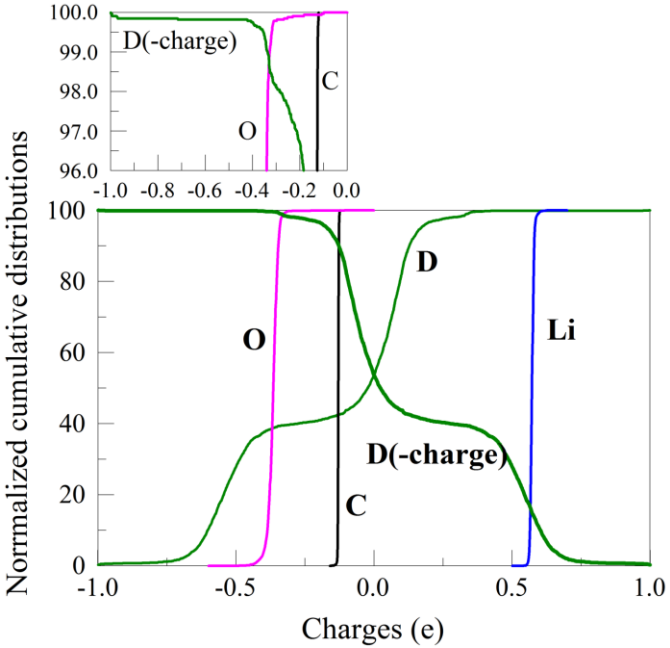

Krstic et al, FE&D, 2011

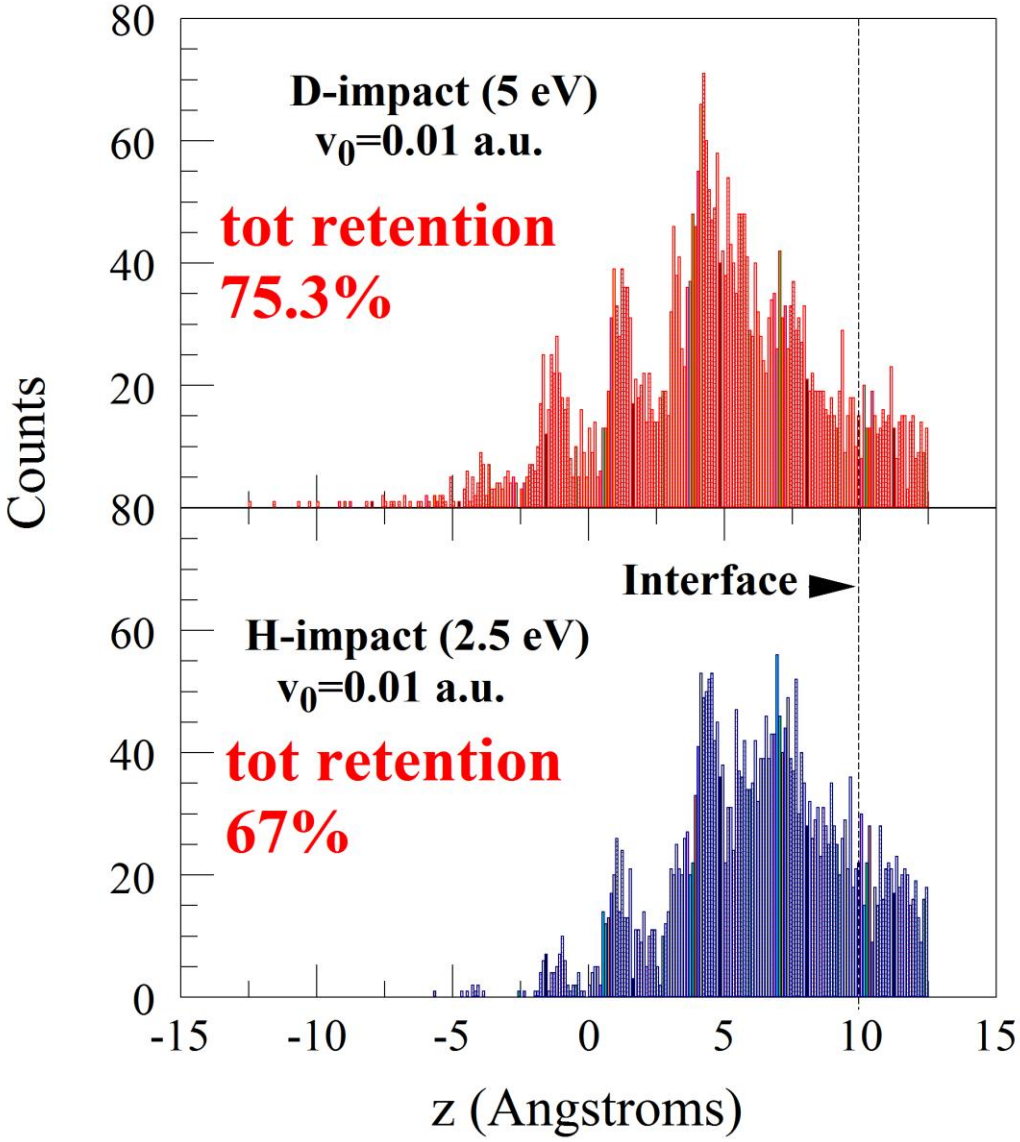

Plasma-Wall Coupling

- Classical effect called “wall pumping” is known since long ago (Cohen et al JNM 76 (1978) 459).

- In short pulse tokamaks, the wall removes significant fraction (>60%) of puffed gas and provides necessary density control in combination with cryopumps.

- In long pulse machines, wall pumping is transitional effect (Loarer et al NF47 (2007) 1112): pumping gradually decreases to zero and then wall condition changes to outgassing triggering MARFE.

- In reaching “global wall saturation” point on JT60U, it was observed:
  - uncontrollable increase in plasma density and formation of MARFE (Asakura et al PPCF 46 (2004) B335)
  - degradation of plasma confinement, ELMs switching from type-I to type-3 (Takenaga et al JNM 337 (2005) 802).

- Theoretical analysis, 0-D (Krasheninnikov et al PoP 13 (2006) 094502) highlighted that plasma contact with highly saturated wall can result in thermal instability of plasma triggering detachment and MARFE formation.

Ocsillations of edge plasma in contact with supersaturated wall

Transitional effects modeled with WALLPSI/EDGE1D include self-sustained oscillations.

Here (+/-) 10-20% variation in recycling coefficient corresponds to transition between MARFE and sheath-limited edge plasmas.

Volumetric pumping is fast enough to pump out the released wall inventory during the MARFE stage.

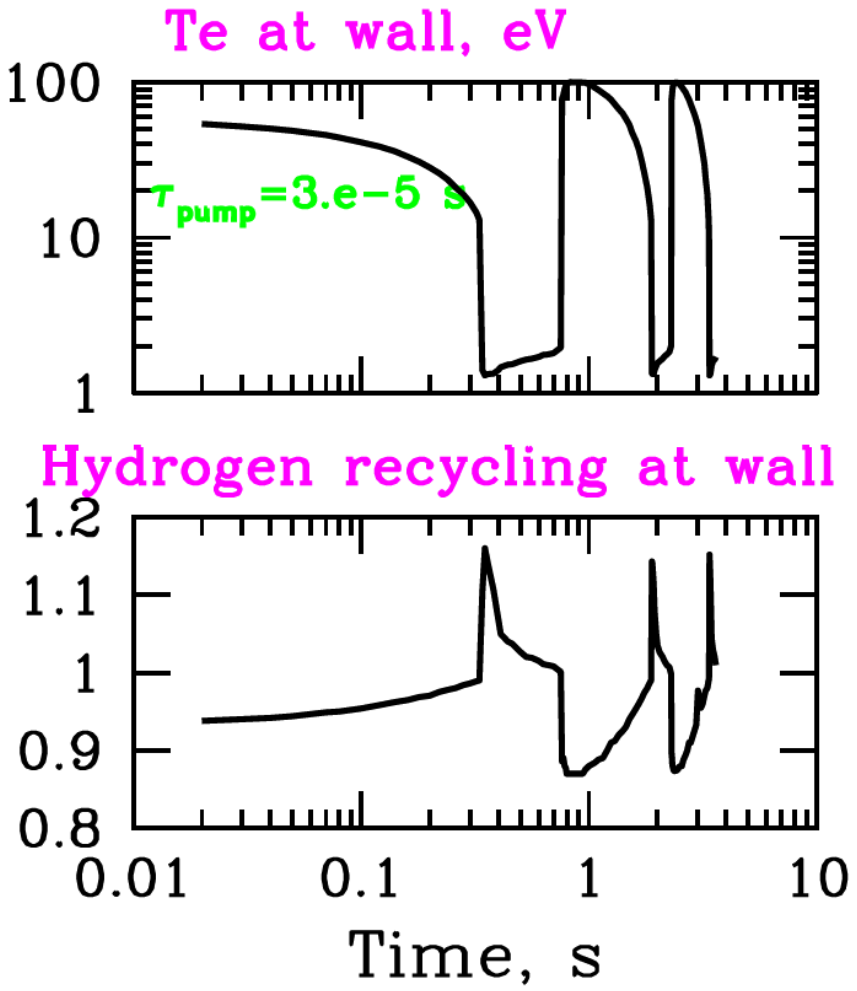

Intermittent edge-plasma transport

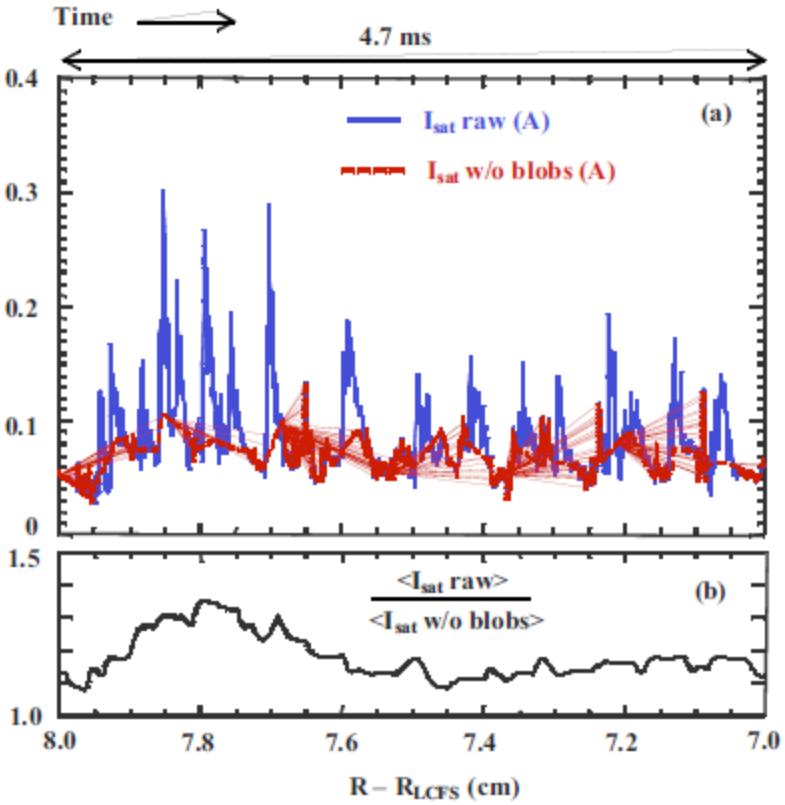

FIG. 1. (Color online) Time trace of the ion saturation current in the far SOL of the DIII-D tokamak plotted against the distance from the LCFS. Shown are: (a) the raw signal of the ion saturation current with blobs (solid line) and processed ion saturation current with blobs removed (dashed line); (b) the ratio of these two signals smoothed over 1 ms.

->Meso-scale structures, blobs, were observed on tokamaks both in L-mode and H-mode between ELMs.
-> They show up as coherent filamentary structures rapidly propagating through the SOL.
->filaments similar to blobs were observed during the ELM and can be modeled in the same way.

-> The resulting cross-field transport is highly intermittent and non-diffusive

->Subject of edge plasma turbulence studies for decade.
-> turbulence code BOUT++ has been developed

-> However, at present, only edge-plasma transport code can handle recycling, atomic physics, impurities etc

Non-diffusive transport models

->Main convective features of non-diffusive transport in transport codes in SOL are provided by combining both anomalous cross-field convective velocity $v_{\perp conv}$ and anomalous cross-field diffusion and heat conduction.

->In particular, convection with ballooning-like poloidal dependence (peaking at the outer mid-plane) significantly improves the comparison of modeling results with data on plasma particle flux on the chamber wall, penetration of impurity into the core, and Mach~1 parallel plasma flows in SOL .

->However, this convective-diffusive approach is still based on the averaged plasma parameters, and it ignores the spatiotemporal features of the intermittency.

-> There is big difference between the time-averaged model and the model resolving the spatiotemporal features of blobby transport, since atomic physics and plasma-wall interactions are strong nonlinear functions $F(\zeta)$, so that, $\langle F(\zeta)\rangle \neq F(\langle\zeta\rangle)$ of a set of fluctuating parameters ζ.

->Edge transport codes assume toroidal symmetry, however blobs break this assumption. Seeded real blobs will momentarily washed out by parallel transport

Macro-blob concept

Blob size δ~0.02m radially and l=qR~6m along field line, volume V= δ^2l~0.0024
For "birth" plasma density N~2x10^{19}/cm3 it contains J=NV~5 x10^{16} D.
For separatrix flux F_{sep}~10^{22}/s, the blob generation rate $\nu=F_{sep}/J$~2x10^5/s.
Blob velocity v=500m/s.
The blob lifetime in SOL is $\tau=L_{sol}/v$~3x10^{-4}s.
Number blobs in SOL M=$\tau\nu$~60

Blobs in SOL are not synchronized, randomly seeded, follow their PDFs.

Combine these blobs into a single toroidally symmetric MACRO-blob.

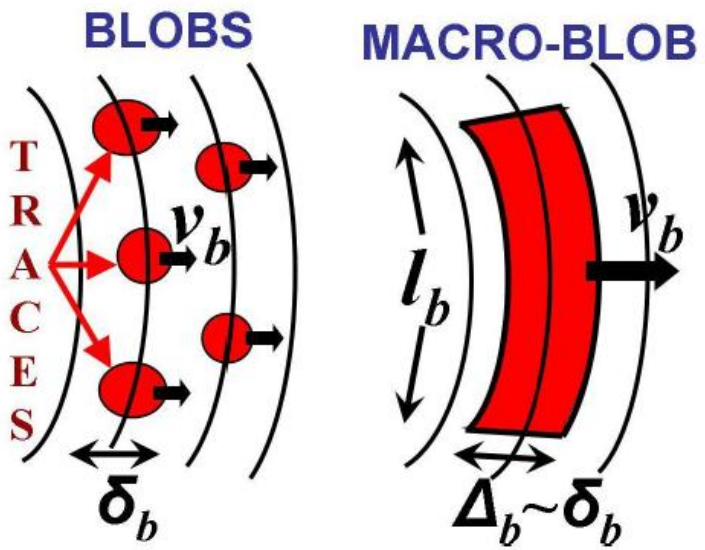

Macro-blob radial size $\Delta=\delta$
Toroidal length $2\pi R$
For pitch angle ψ~0.1
Poloidal length $L_{mb}=qR\psi$~0.6m
Volume V_{mb}~0.15m3
$V/V_{mb}=60=M$
Macroblob generation frequency is
$\nu_{mb}=\nu M$

Macroblob is larger than ordinary one in volume but correspondingly infrequent

Macroblob model in UEDGE

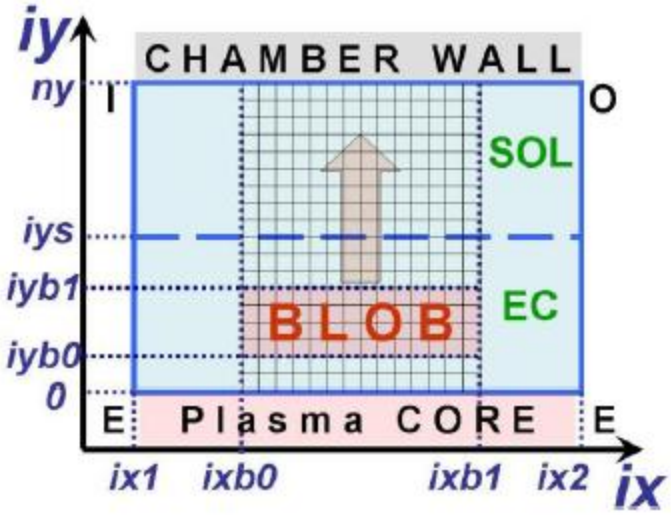

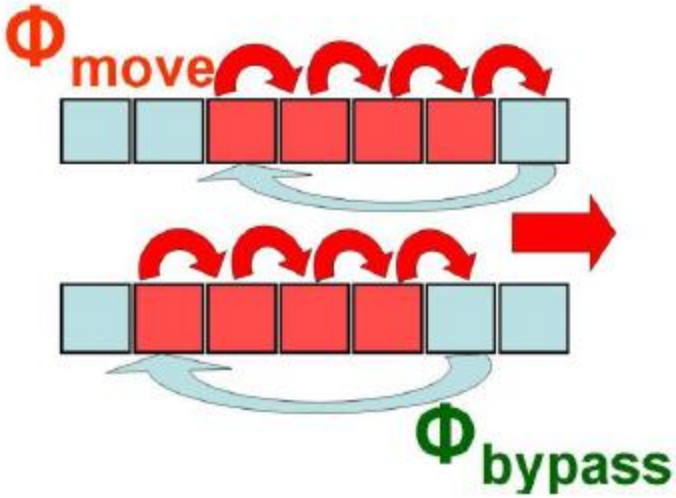

Seed the macroblob on mesh according to PDF

Assign the radial velocity to blob cells

Use sink/source terms to advance blob coherently in time toward the wall

Move background plasma discontiniously in opposite direction

Solve usual plasma transport equations

Single Macroblob dynamics

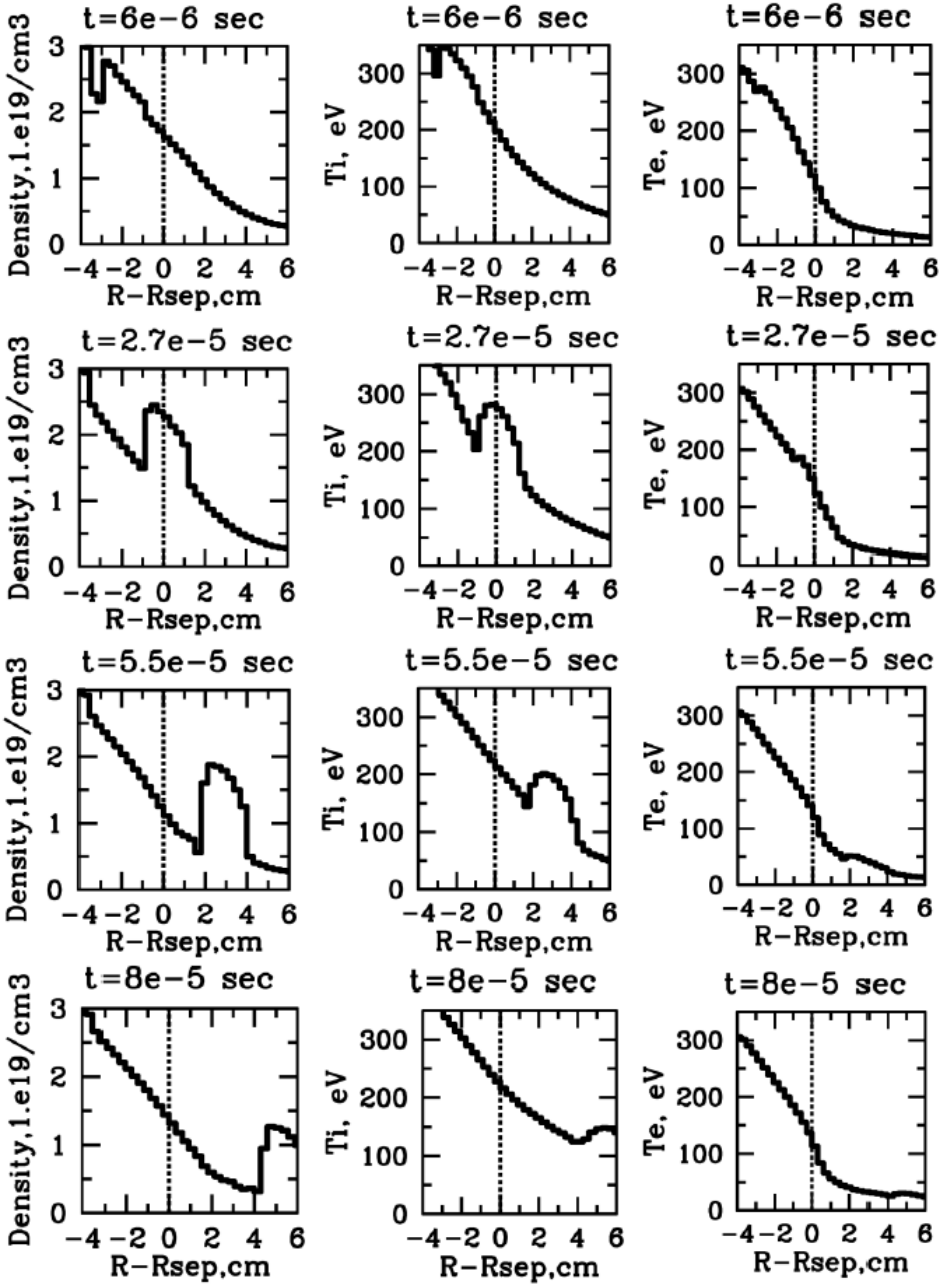

Single macro-blob dynamics (Cont.)

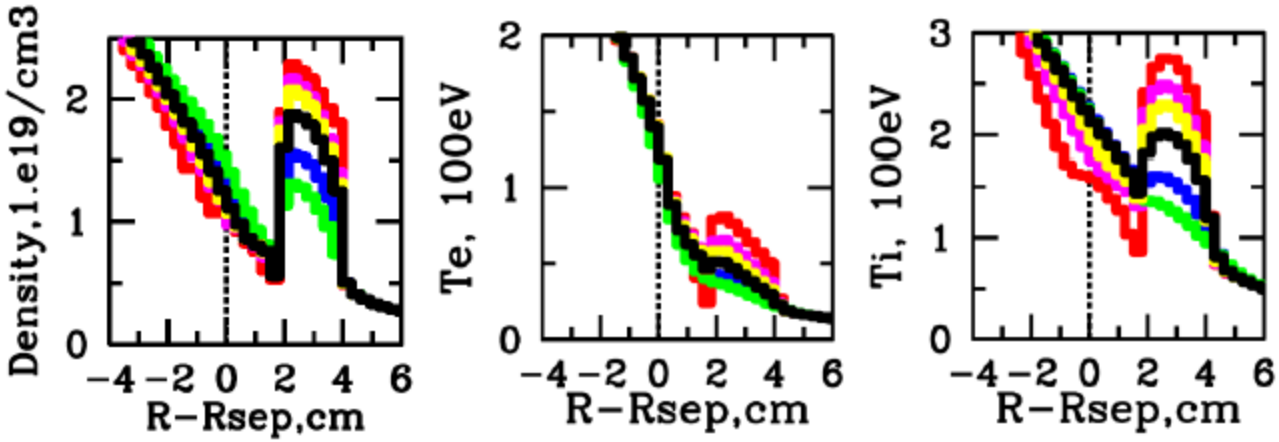

The higher is the blob velocity, more plasma particles and heat go to wall

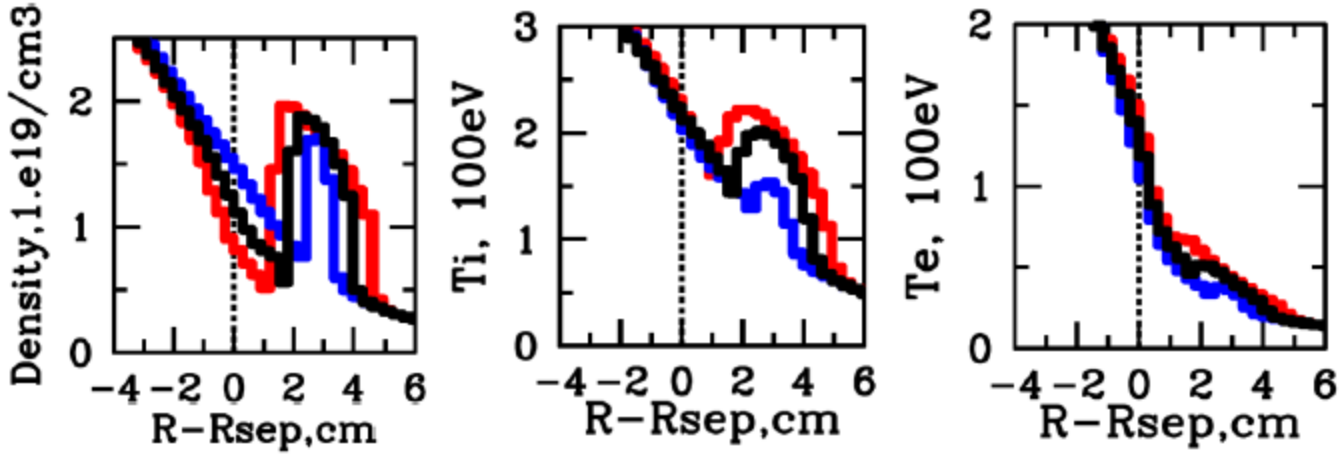

The larger is the blobs, the slow is its decay

Macroblob impact on wall

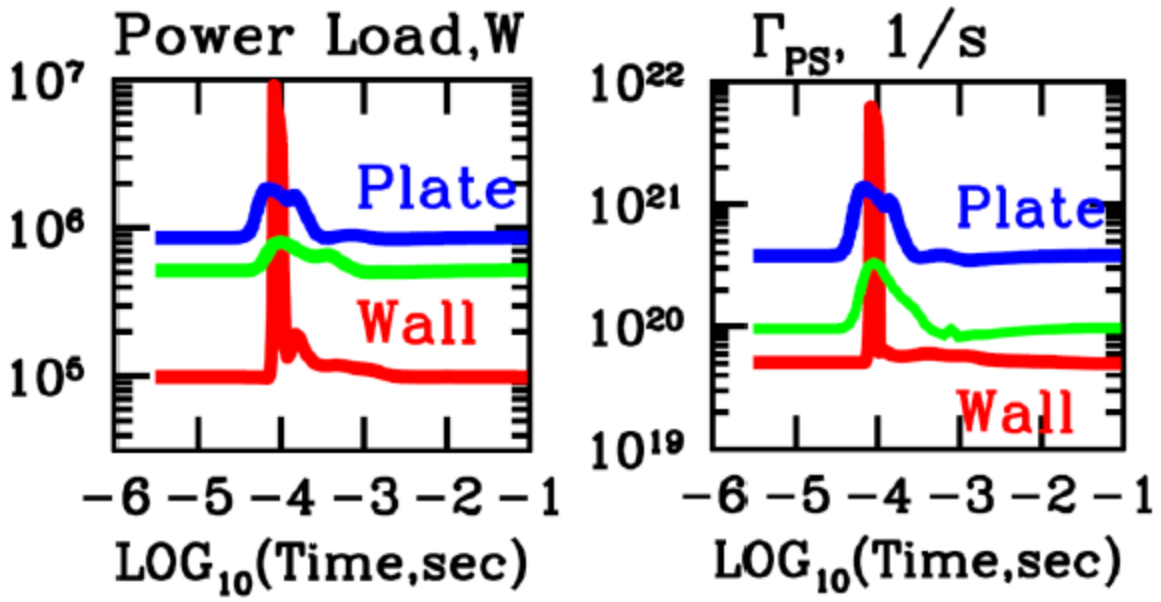

High transient power load and sputtering on all surfaces

Effect of blob on plasma particle balance

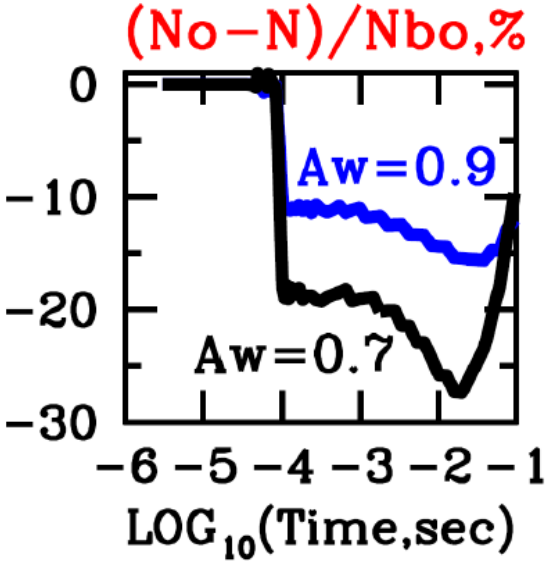

Wall pumps (1-A_w) fraction of particles arrived on wall with blob N_{bw}
A_w fraction of N_{bw} momentarily goes into the core
The particles deposited by blob into divertor ~N_{bo}-N_{bw} are mostly pumped there at 100 ms time scale and not going to core because of high recycling
So flux to core increases, while divertor increasingly pumps

Modeling of quasi-stationary conditions with a sequence of macroblobs by adjusting background plasma diffusivities is in progress

Enhanced wall erosion and inward transport of impurities by blobs

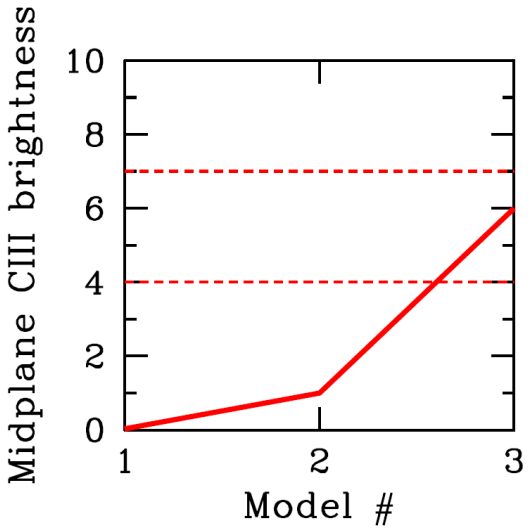

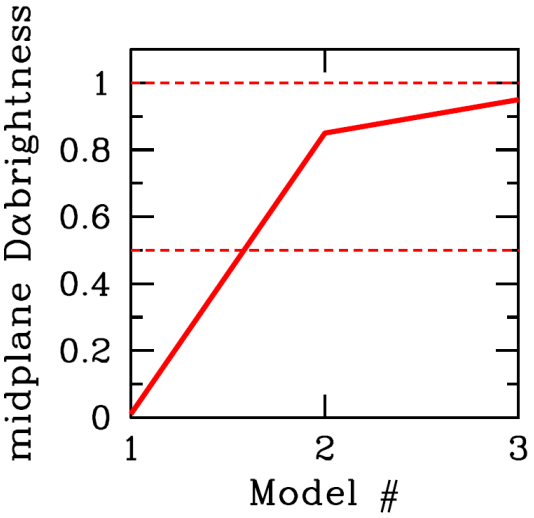

Model #1 Pure diffusive transport
Model #2 Ad hoc convective transport
Model #3 Macroblobs

Modeling for the same DIII-D SAPP discharge

As expected although models #2 and #3 match midplane recycling, only macroblob #3 model can explain impurity concentrations.

Important effect is that macroblobs while traveling in SOL also advance low charge states of impurities towards the core plasma, whereas high charge states it deposits to wall causing self-sputtering.

Conclusions

Dynamic models for plasma-wall interactions has been reviewed. Underline theory for macroscopic transport model, classical Molecular Dynamic model and Tight Biding DFT model was discussed. Recent progress as well as existing gaps were highlighted.

Results on macroscopic modeling of deuterium recycling, chemistry, retention and sublimation for beryllium were presented. Creation of supersaturated layer is an important feature of plasma-wall interactions which can explain available experimental results.

Results on classical MD modeling of sample evolution to supersaturated conditions as well as dependence of SSL CHS on surface temperature, sputtering yields and characteristics of ejected particles were given.

New “macro-blob” model for plasma-wall interactions under intermittent edge-plasma transport and ELMs was discussed and modeling results for DIII-D discharges were presented.